



Seismic response of a bridge structure with controlled rocking tubular steel piers

Robert Tremblay¹, Julie Liu², Kamrul Islam³, Ahmad Rahmzadeh⁴, and M. Shahria Alam⁵

¹ Professor, ²M.Eng. Student, ³PhD Student, Department of Civil, Geological and Mining Engineering, Polytechnique Montreal, Montreal, QC, Canada.

⁴PhD Student, ⁵Associate Professor, Department of Civil Engineering, University of British Columbia, Okanagan, BC, Canada.

ABSTRACT

The use of controlled rocking bridge piers has attracted interest to achieve enhanced seismic performance for bridge structures. Most past research on the system has focused on reinforced concrete columns. This article examines the application of the system to tubular steel columns. The system relies on gravity load and post-tensioned (PT) elements for re-centering capacity and yielding or friction energy dissipation (ED) mechanisms for the control of lateral displacements. Rocking interfaces and ED elements are used at the top and bottom ends of the columns. After a severe earthquake, bridges with such rocking piers are expected to return to their original position with no or minor structural damage. Equations are proposed to select the column size and characteristics of the PT and ED elements that are required to achieve the desired lateral load-displacement response. A numerical model capable of reproducing the hysteretic response of the column using commercially available structural analysis programs is presented. The model is then used to examine the longitudinal seismic response of a two-span bridge located in Vancouver, BC. Friction ED was considered for the bridge studied. Nonlinear dynamic analysis was performed under an ensemble of 33 representative ground motions and the results show that the proposed system can effectively control lateral displacements and mitigate residual deformations of the structure. The rocking response of the piers induces vertical dynamic response of the superstructure, which leads to additional axial loads in the columns. A parametric study was conducted to evaluate the impact on the bridge seismic response of varying the column diameter, the ED frictional resistance, and the initial tension and number of tendons for the PT element. The results indicate that the first two parameters have the greatest impact. The influence of vertical ground motions was examined for a subset of 11 records. Vertical shaking has negligible effects on the bridge lateral response but slightly increases the vertical dynamic response of the superstructure.

Keywords: Controlled rocking, Self-centering, Friction, Steel Bridge Pier, Post-tensioning

INTRODUCTION

Devastating recent earthquakes have inspired researchers to develop new and improved structural systems with seismic resilience. In this context, self-centering structures have garnered popularity among researchers due to their ability to minimize structural damage and return to their original position after strong earthquakes. Rocking bridge pier has been proposed for the seismic design and retrofit of bridge structures and notable projects were completed where rocking response was introduced in the bridge piers for enhanced seismic performance, including the South Rangitikei Railway Bridge in New Zealand, the North Approach of the Lions' Gate Bridge in Vancouver, and the Wigram-Magdala Link Bridge in New Zealand [1-3]. Controlled rocking piers generally rely on gravity load and post-tensioned (PT) tendons to develop a flag-shaped hysteretic response that results in a stable and self-centering seismic response. Energy dissipation (ED) elements are typically provided at the rocking interfaces to control the bridge displacements. The system can be designed and detailed to eliminate or reduce considerably residual displacements and structural damage. In addition, in recent years, the bridge engineering community in North America has been seeking to develop accelerated bridge construction (ABC) strategies to reduce construction time and traffic congestion. The concept of prefabricated rocking bridge piers represents a suitable solution to both challenges related to post earthquake functionality and rapid construction.

Past experimental and numerical work on rocking/self-centering bridge piers mainly focused on reinforced or prestressed concrete piers [e.g., 4-8]. The seismic response and design of rocking steel trussed piers was also examined [9] and studies were conducted on composite circular columns and I-shaped steel columns [10-11]. A research was initiated recently to investigate the possibility of using circular steel tubes as rocking bridge piers. The columns would be detailed with steel end plates, PT tendons and yielding- or friction-based ED devices placed at the rocking joints. A numerical study showed that such rocking tubular columns can perform well and display stable hysteretic flag-shaped response under reversed cyclic loading,

provided that column local buckling is prevented by means of proper section slenderness limits and adequate end details [12]. However, no study has examined the seismic response of bridge structures with rocking columns made from hollow steel tubes. This article presents equations that can be used to predict the lateral load-displacement response of rocking steel columns built with PT and ED elements. The rocking steel column system is then applied for the seismic resistance of a simple two-span reference bridge structure located in Vancouver, British Columbia. The response of the bridge columns is described. The seismic response of the structure is investigated through nonlinear response history analysis (NLRHA). A parametric study is performed to evaluate the influence of key design parameters on the seismic response of the bridge structure. The influence of vertical ground motions is also investigated.

PREDICTION OF THE LOAD-DISPLACEMENT RESPONSE OF ROCKING BRIDGE PIERS

The rocking bridge column studied is illustrated in Figure 1a. It consists in a steel circular tubular column with circular top and bottom end plates. The column has axial stiffness EA_c , flexural stiffness EI_c , and height, h_c . Rocking is intended to occur at the top and bottom column ends against steel plates inserted in the foundation at the base and placed underneath the superstructure at the top (Figure 1b). The PT elements are unbonded steel tendons with axial stiffness EA_t and initial pre-tension force T_i placed at the center of the column. Yielding or friction ED elements with resistance F_s are used at the rocking interfaces.

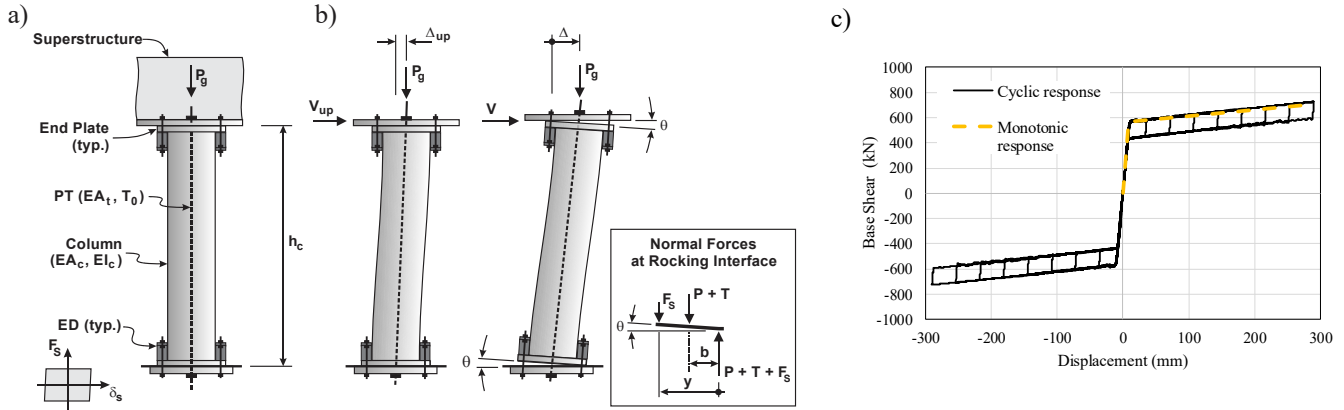


Figure 1. Rocking column: (a) At rest; (b) Under V_{up} and after rocking; (c) Lateral load-displacement response.

Post-tensioning is expected to be performed before the installation of the superstructure; hence, the available pre-tension at the time of the earthquake will be reduced from T_i to T_0 due to the bridge self-weight P_g :

$$T_0 = T_i - \frac{P_g}{1 + E_c A_c / E_t A_t} \quad (1)$$

Prior to rocking, the column is rigidly connected at its both ends and has an initial lateral stiffness K_0 . For simplicity, the flexural stiffness of the superstructure is assumed to be large compared to that of the column and the rotation of the superstructure at the top end of the column is set equal to zero. The column lateral stiffness can then be approximated as $K_0 = 12EI_c/h_c^3$ and the rotation θ at top and bottom rocking interfaces are assumed to be equal.

Once rocking has initiated, the overturning moment caused by the lateral load V and the vertical load P_g is resisted by the flexural resistance at the two rocking interfaces that results from gravity load P_g , the tension force T in the PT element and the resistance F_s of the ED elements (see Figure 1b):

$$Vh_c + P_g \Delta = 2(P_g + T)b + 2 \sum F_{s,i} y_i \quad (2)$$

In this equation, b is the horizontal distance between the column centerline and the point of rotation at the rocking interfaces and y_i is the horizontal distance between each ED device and the rocking point. The multiplier 2 is applied to the terms on the right-hand-side of the equation to include the contribution to moment resistance from the two rocking interfaces. The lateral displacement Δ is due to the elastic deformation of the column and rotation at the rocking interfaces θ :

$$\Delta = \frac{V}{K_0 - P/h_c} + \theta h_c \quad (3)$$

In Eq. (3), the column lateral stiffness K_0 is reduced to account for P-delta effects ($K_0 - P/h_c$). Introducing this expression in Eq. (2) gives:

$$Vh_c + P_g \left(\frac{V}{K_0 - P_g/h_c} + \theta h_c \right) = 2(P_g + T)b + 2 \sum F_{s,i}y_i \quad (4)$$

$$\Rightarrow V = \left(1 - \frac{P_g}{K_0 h_c} \right) \left[\frac{2(P_g + T)b + 2 \sum F_{s,i}y_i}{h_c} - P_g \theta \right] \quad (5)$$

The tension load T in the PT tendons is equal to the initial tension T_0 plus the increment due to the tendon elongation caused by the rotation θ at the rocking interfaces:

$$T = T_0 + \frac{2 \theta b EA_t}{h_c(1 + EA_t/EA_c)} \quad (6)$$

For a given θ , T is obtained from Eq. (6) and V is determined from Eq. (5). The corresponding value of Δ is then calculated from Eq. (3). At initiation of rocking, $\theta = 0$ and $T = T_0$ and the lateral load causing rocking, or column uplift, V_{up} , is given by:

$$V_{up} = \left(1 - \frac{P_g}{K_0 h_c} \right) \left[\frac{2(P_g + T_0)b + 2 \sum F_{s,i}y_i}{h_c} \right] \quad (7)$$

The corresponding lateral displacement Δ_{up} is determined with $V = V_{up}$ in Eq. (3). To prevent failure of the PT element, the tension from Eq. (6) must be limited to some fraction β of T_u , which gives the rotation capacity of the rocking interfaces, θ_{max} :

$$\theta_{max} = (\beta T_u - T_0) \frac{h_c(1 + EA_t/EA_c)}{2 b EA_t} \quad (8)$$

The maximum lateral load and displacement corresponding to θ_{max} , V_{max} and Δ_{max} , are calculated with $T = \beta T_u$ and $\theta = \theta_{max}$ in Eqs. (3) and (5). The complete backbone response of a given rocking column up to maximum displacement can then be established using the above equations.

DESIGN AND GEOMETRY OF ROCKING BRIDGE PIER

The bridge studied is a two-span straight overpass bridge located on a class C site in Vancouver, British Columbia. The superstructure includes four continuous composite steel girders. As illustrated in Figure 2a, the girders at the intermediate support are connected to an integral steel cap girder supported on two 800 mm diameter rocking steel columns. The columns are 5.4 m in height and are detailed to rock at both ends along both orthogonal directions. This study is, however, limited in scope to evaluating seismic response in the longitudinal direction.

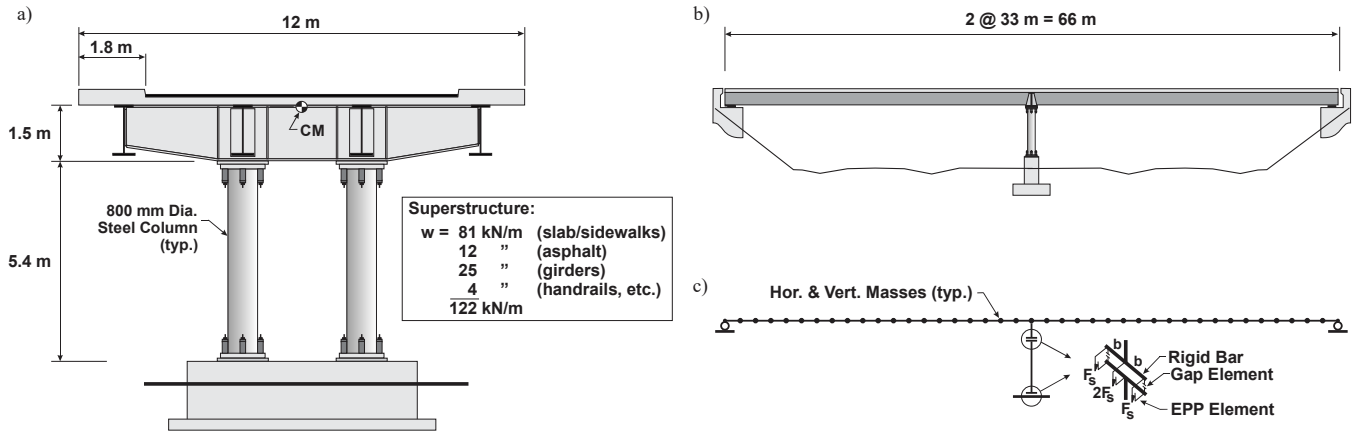


Figure 2. Studied two-span bridge: (a) Cross-section at intermediate support; (b) Bridge elevation; and (c) Numerical model.

The columns are made from ASTM A252, Grade 3, steel pipes with a specified yield strength $F_{yc} = 310$ MPa and Young's modulus $E_c = 200000$ MPa. The tube wall thickness is 25 mm, which gives $A_c = 60870$ mm², $I_c = 4570 \times 10^6$ mm⁴, and a column initial stiffness $K_0 = 69.7$ kN/mm. The tubes have a diameter-to-thickness ratio of 32, a value sufficiently low to prevent local buckling upon rocking from the previous study [12]. The columns include welded 1000 mm diameter top and bottom end plates.

Friction ED elements with a slip load of 100 kN each are placed at both ends of the columns at 90° intervals along the circumference of the columns. The axial load per column from dead load is 2510 kN. The PT element for each column consists of seven ASTM A416, 15 mm diameter (140 mm²) 7-wire strands with ultimate tensile stress $f_{pu} = 1860$ MPa and $E_t = 195000$ MPa. The tendons were pretensioned at $0.3 f_{pu}$, giving $T_i = 547$ kN. From Eq. (1), the tension in the PT tendons reduced to $0.28 f_{pu}$ ($T_0 = 510$ kN) due to elastic losses upon application of the load P . The total column axial load under the dead load is therefore 3020 kN, i.e., 16% of the column yield resistance $P_y = A_c F_y$ (18870 kN).

To estimate the column lateral response, the distance b is set equal to 450 mm, i.e. slightly less than half the diameter of the end plates recognizing that the plates will likely experience some bending upon rocking bend [12]. The distance y_i takes a value of 450 mm for the two ED devices positioned at 90° from the rocking point, and 900 mm for the device located on the opposite side of the tube. With these values in Eq. (7), the load V_{up} for each column is 567 kN and $\Delta_{up} = 8.2$ mm. A value of β equal to 0.7 was adopted for this bridge and θ_{max} from Eq. (8) is equal to 0.0245, which gives $V_{max} = 632$ kN and $\Delta_{max} = 141$ mm. The latter value corresponds to 2.6% of the column height and the expected vertical slip in the friction ED mechanisms at θ_{max} is 22 mm, which can be easily accommodated. Figure 1c shows the lateral load-deformation obtained with these values. As shown, the column exhibits a positive stiffness upon rocking, $K_r = 0.50$ kN/mm.

For this bridge, the total weight of the superstructure is 8052 kN (122 kN/m x 66 m), i.e. 4026 kN per column. With $K_0 = 69.7$ kN/mm, the period in the longitudinal direction is 0.48 s. For the site considered, the design spectral acceleration specified at this period for a probability of exceedance of 2% in 50 years in the CSA S6 standard [13] is 0.758 g. The elastic force demand would therefore be 0.758×4026 kN = 3052 kN and $V_{up} = 567$ kN would suggest an equivalent R factor of 5.4, which appears reasonable. The design spectral displacement demand for $T = 0.48$ s is 43 mm, well below $\Delta_{max} = 141$ mm. This displacement demand is however based on 5% viscous damping and assumes equal displacements in the linear and nonlinear ranges, which may not be applicable to a rocking, self-centring system exhibiting limited damping. More comprehensive NLRHA is needed to obtain a more reliable estimate of the bridge seismic displacement response, as is done in the next section.

The column size was also validated for other seismic and non-seismic load combinations. For instance, member strength and stability were checked under 1.25 times the dead load (D) and 0.5 times the traffic live load (L) plus the additional axial load and moments at Δ_{max} . The 1.25 dead load factor is specified in CSA S6 to account for vertical acceleration effects whereas 0.5 L was considered in anticipation of possible traffic congestions in a metropolitan area during a severe earthquake. Member strength and stability were also verified under total factored dead load and traffic live load, and the rocking capacity of the columns resulting from T_0 and unfactored (1.0) dead load was checked against the overturning moment imposed by factored (1.7) longitudinal braking load.

SEISMIC RESPONSE OF THE BRIDGE STRUCTURE

Numerical model

The bridge structure was analyzed using a commercially-available computer program [12]. The model used is illustrated in Figure 2b. Since the study was limited to the longitudinal response, the model included one column and half the superstructure width. The column and superstructure were represented by elastic frame elements. Rigid frame elements were used with gap elements with high compression stiffness and zero tension stiffness to reproduce the rocking interfaces. Elastic-perfectly plastic (EPP) nonlinear link elements were employed to reproduce the friction ED devices. Longitudinal constraints were imposed between rocking interfaces to avoid sliding. The superstructure was discretized with 20 frame elements per span and the tributary masses of the superstructure were assigned to all nodes in the vertical and horizontal directions. Mass was also assigned to the column frame elements and the rigid bars forming the rocking interfaces. As shown, rollers were provided at the abutments such that the horizontal seismic resistance along the longitudinal direction was entirely provided by the rocking pier. Periods and mode shapes in the first three modes are presented in Figure 3. Rayleigh damping corresponding to 3% of critical in the first and third modes was assigned to the model, with stiffness proportional damping assigned only to the material of the frame elements to avoid the development of excessive damping forces in the nonlinear link elements. The model did not include any gravity loads; a vertical acceleration of 1.0 g was imposed in all analyses to generate gravity load effects from the structure masses. Second-order analysis was also performed to include P-delta effects.

In Figure 3a, the first mode shape involves flexural deformations of the superstructure, contrary to the infinitely stiff superstructure assumption made in the calculation of K_0 and the derivation of Eqs. (1) to (8). This higher flexibility explains the longer bridge fundamental period obtained from analysis (0.56 s) compared to the estimated value of 0.48 s determined with the stiffness K_0 . Prior to performing the NLRHA, cyclic nonlinear static analysis under stepwise incremented displacements was performed to validate the bridge model and the hysteretic response is plotted in Figure 1c. Despite the difference in initial stiffness, the predicted backbone response from Eqs. (1) to (8) compares very well with the analysis predictions. As expected, the computed hysteresis displays a symmetrical flag shape typical of full self-centering systems.

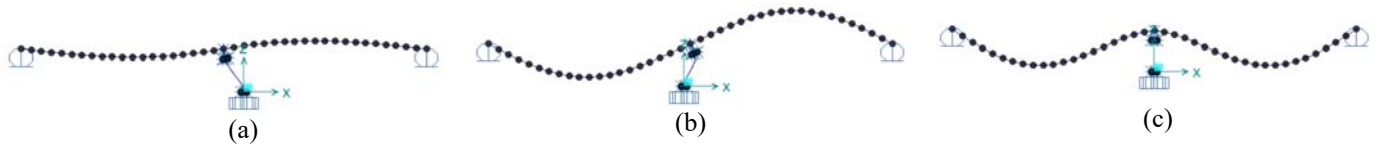


Figure 3. Bridge modal properties: (a) Mode 1 - $T_1 = 0.56$ s; (b) Mode 2 - $T_2 = 0.30$ s; and (c) Mode 3 - $T_3 = 0.22$ s.

Selection and scaling of seismic ground motions

Nonlinear response history analysis was performed using an ensemble of 33 representative horizontal seismic ground motions selected and scaled in accordance with the guidelines of Commentary J of the 2015 National Building Code of Canada [15]. The ensemble comprises 3 suites of 11 ground motion records, one for each of the three earthquake sources contributing to the hazard for the site: shallow crustal, subduction deep in-slab, and subduction interface earthquakes. Figure 4a shows the acceleration spectra of the scaled horizontal ground motion records. The effect of vertical ground motions will be studied in the last section of the paper. For this study NLRHA is performed for the suite of 11 crustal earthquake ground motion records by applying simultaneously the horizontal and vertical ground motion components. In these analyses, the vertical ground motion components are scaled using the scaling factors determined for the geomean values of the two horizontal components of the ground motion records. Spectra of these records are shown in Figure 4b.

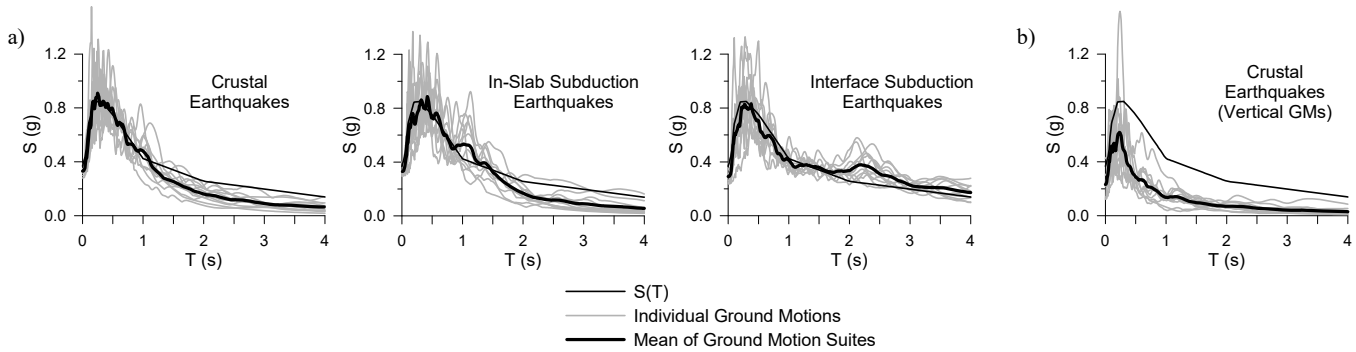


Figure 4. 5% damped acceleration spectra of: (a) Suites of 11 scaled horizontal ground motion records from crustal, in-slab subduction and interface subduction earthquakes; (b) Suite of 11 scaled vertical ground motions from crustal earthquakes.

Seismic Response of the reference bridge

The seismic response of the reference bridge under a crustal earthquake horizontal ground motion record is shown in Figure 5. Full and partial time histories are presented for four response parameters. For this ground motion, the peak horizontal displacement reaches 109 mm, i.e., 2.0% h_c , and the structure eventually returns to its original position at the end of the earthquake, with no residual displacement. The second pair of plots show the variation of the tension in the tendons during the ground motion. The initial tension is equal to T_0 ($= 510$ kN). Under the large displacement cycles, the tension force increases when opening of the rocking interfaces occurs. The maximum tension in the PT element goes up to 1090 kN which corresponds to 60% of T_u . The third pair of plots depict the vertical acceleration of the superstructure at the pier location. Acceleration peaks reaching up to nearly 3g develop each time the pier returns to its original position after rocking has occurred. This impact response induces a vertical dynamic response associated to the third (vertical) mode of the bridge structure. The fourth pair of time history plots present the axial compressive load in the steel column. The observed oscillations are induced by the variations in the PT force due to rocking combined with the effects of the dynamic vertical response of the superstructure. Initially, the column compression is 3020 kN as per design. During the ground motion, it varies from 2580 kN to 4090 kN. The maximum increase in the PT element tension ($1090 - 510 = 580$ kN) can only augment column compression up to 3600 kN; the fact that the compression decreases below 3020 kN and exceeds 3600 kN is caused by the superstructure vertical vibration response.

For each response parameter, the seismic design value used to assess the bridge seismic response is the largest of the three mean values computed for each suite of ground motions. For the reference bridge structure, these values are: peak displacement of 128 mm (2.4% h_c), peak tension load of 1192 kN in the PT tendons and peak column compression load of 4150 kN. In addition, the peak slip distance in the ED elements is 18 mm. No residual deformations were observed in the analyses. The peak displacements exceed the spectral value obtained with the period based on K_0 , indicating that a more appropriate method is needed for this system. Nevertheless, the computed peak displacements are within the displacement capacity of the rocking column and all other response parameters would result in satisfactory behaviour. These findings show that the rocking bridge pier system can be effectively used to achieved controlled seismic response and superior bridge performance.

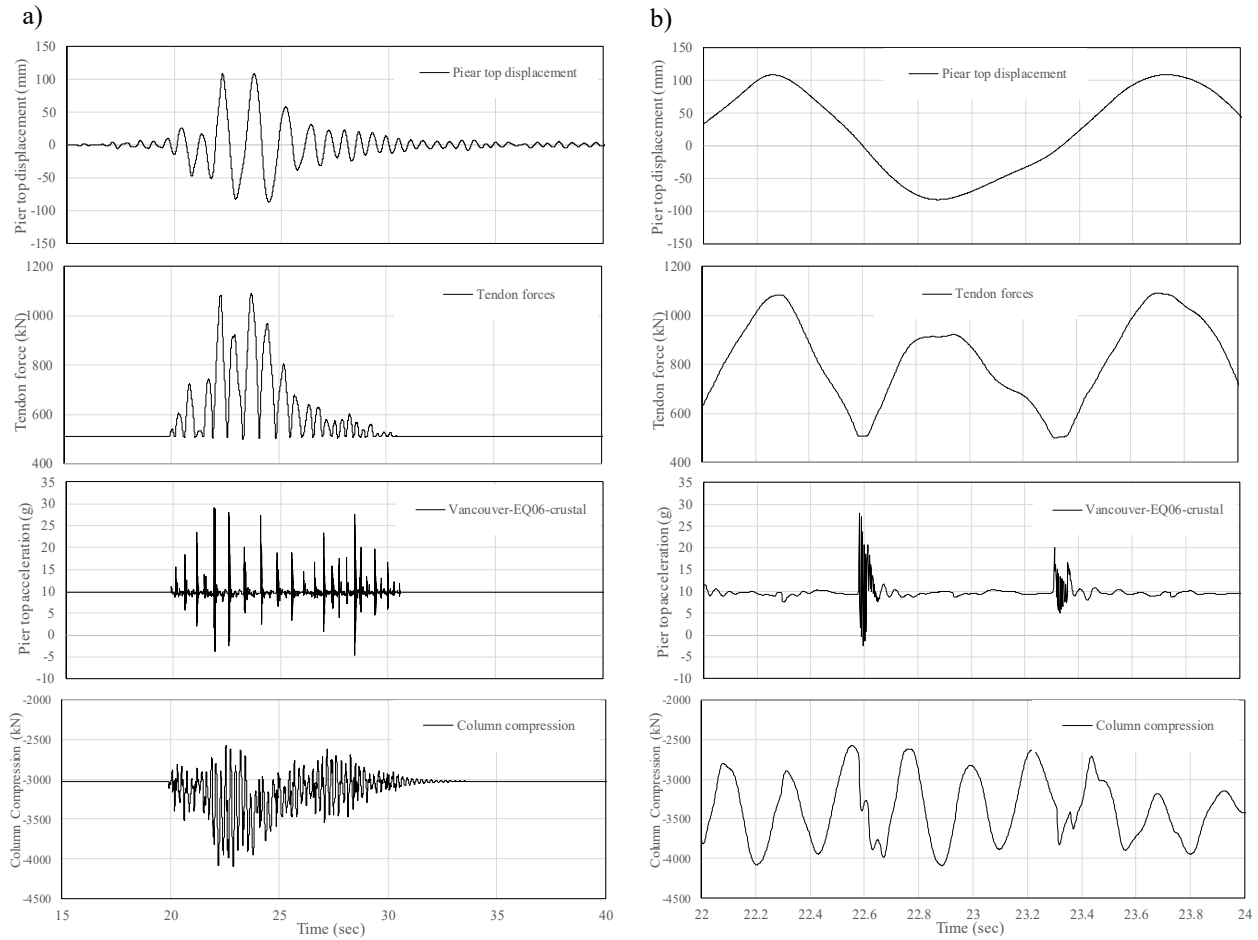


Figure 5. Time histories of the bridge long. displacement, tension load in PT, vertical acceleration at pier top, and column compression load under a crustal ground motion event: (a) Entire response; (b) Close-up response for the 22-24 s window.

Parametric study

A parametric study was performed to investigate the effects of key design parameters on the seismic response of the bridge studied. The four varied parameters are listed in Table 1. For each one, three cases are considered. The B configuration corresponds to the reference bridge studied in the previous section, whereas cases A and C are obtained by reducing and increasing, respectively, the values of the varied parameters. A total of 9 different column designs are therefore investigated, and key parameters defining their lateral properties are given in Table 2. Increasing the column diameter increases the stiffness K_0 , reduces the fundamental period, and increases the stiffness K_r upon rocking. However, these three parameters are not affected by F_s , T_0/T_u and n_t . Increasing D , F_s , T_0/T_u or n_t always results in a higher lateral load at uplift, V_{up} . The value of θ_{max} , as limited by the maximum PT stress $0.7f_{pu}$, is reduced when increasing the column diameter and the T_0/T_u ratio.

The results of the NLRHA performed on the 9 different structures under the 33 horizontal ground motion records are presented in Table 3. The results clearly show that increasing the pier diameter or the ED element capacity has the strongest positive impact on the bridge lateral displacements. An increase in the ED slip load also has a beneficial effect on the peak tension load in the tendons and peak compression load in the steel column. Conversely, reducing the column diameter has the worst effect on lateral displacements, peak compression load in the column and peak tension in the PT element. As shown, increasing the initial tension or the number of tendons in the PT element has nearly no effect on the bridge displacements. This is likely because the contribution of the PT element to the column lateral stiffness is small. In addition to negatively affecting θ_{max} (in Table 2), an increase of the initial tension in the tendons (case C3) also leads to significantly higher axial forces in the column and the tendons. Reducing the number of tendons in case A4 appears as a good strategy to reduce the peak tension in the PT element and the column compression loads without detrimentally affecting the bridge longitudinal displacements.

Table 1. Varied parameters

	A	B (Reference)	C
1. Column diameter, D (mm)	640	800	1000
2. Slip load of the energy dissipation elements, F_s (kN)	50	100	200
3. Initial prestressing stress, T_0/T_u	0.23	0.28	0.48
4. Number of prestressing strands, n_t	5	7	9

Table 2. Properties of the bridge structure for the 9 configurations studied.

	A1	B	C1	A2	B	C2	A3	B	C3	A4	B	C4
K_0 (kN/mm)	34.9	69.7	139	69.7	69.7	69.7	69.7	69.7	69.7	69.7	69.7	69.7
T_1 (s)	0.68	0.48	0.34	0.48	0.48	0.48	0.48	0.48	0.48	0.48	0.48	0.48
K_r (kN/mm)	0.18	0.50	0.98	0.50	0.50	0.50	0.50	0.50	0.50	0.50	0.50	0.50
V_{up} (kN)	461	567	696	533	567	633	551	567	627	542	567	591
θ_{max}	0.030	0.025	0.020	0.025	0.025	0.025	0.027	0.025	0.013	0.024	0.025	0.025

Table 3. Peak values of response parameters of the 9 configurations studied

	A1	B	C1	A2	B	C2	A3	B	C3	A4	B	C4
Δ (% h_c)	4.5	2.4	1.8	2.9	2.4	2.0	2.4	2.4	2.3	2.5	2.4	2.5
P (kN)	4419	4150	4360	4383	4150	4045	4062	4150	4546	3885	4150	4557
P/P_y (%)	30	22	18	23	22	21	22	22	24	21	22	24
T (kN)	1568	1192	1157	1351	1192	1081	1112	1192	1550	886	1192	1568
T/T_u (%)	86	65	63	74	65	59	61	65	85	68	65	67
ED Slip (mm)	29	18	17	22	18	15	19	18	18	20	18	19

Effect of vertical ground motions on the bridge response

The effect of vertical ground motions is studied using the ensemble of 11 ground motion records from crustal earthquakes. Mean results without and with the vertical ground motion components are given in Table 4. Vertical ground motions have negligible effects on the bridge lateral displacements and, thereby, the tension force in the PT element and displacements in the ED devices. However, they induce 19% higher peak axial compression loads in the steel column and 27% larger negative bending moments in the bridge girders at the pier location. When compared to the static values, negative moments in the girders were increased by 1.52 due to impacts upon rocking under horizontal ground motions. When considering vertical ground motions, this flexural demand amplification reaches 1.94. Such vertical ground motion effects on column axial loads and girder moments are attributed to the bridge superstructure dynamic vertical response.

Table 4. Mean response parameters for the reference bridge under crustal earthquake ground motions.

	Horizontal ground motions	Horizontal and vertical ground motions
Δ (% h_c)	1.93	1.97
P (kN)	4062	4819
T/T_u (%)	58	59
ED slip (mm)	14	15
M (kN-m)	12540	15970
M/M_{static}	1.52	1.94

CONCLUSIONS

This paper introduced controlled rocking bridge piers built with circular steel tube sections. Equations were proposed to predict the lateral load-deformation response of the piers up to its lateral deformation capacity. The concept was then applied to a two-span bridge located on site class C in Vancouver, British Columbia. NLRHA of the structure was performed under an ensemble of 33 representative ground motion records to examine the bridge seismic response in its longitudinal direction. The bridge model included the rocking column as well as the superstructure to examine the vertical dynamic response due to the rocking response. The column diameter, the ED slip resistance, and the initial tension and number of tendons in the PT element were varied to examine the influence of these variables on the bridge response. Analyses were also conducted using a subset of 11 ground motion records that included the vertical components. The following conclusions can be drawn from this study:

- The use of steel rocking piers for bridge structures can effectively control the structure lateral displacements and avoid structural damage and residual deformations. However, impacts due to column rocking induce vertical dynamic response of the bridge and additional column axial loads that must be considered in the structure design.
- Increasing the column diameter or the ED resistance is the most effective approach to reduce bridge displacements. Varying the initial PT force or the number of post-tensioned tendons has marginal effects on the bridge lateral response. Increasing the initial tension in the tendons leads to higher axial loads in the column and the PT element. Reducing the number of tendons reduces the peak tension in the tendons and the column compression loads without detrimentally affecting the bridge displacements.
- The vertical ground motions have no significant effect on the bridge lateral response, but they induce greater vertical dynamic response of the superstructure and, thereby, amplify further axial loads in the columns and forces in the superstructure.

Further studies are needed to develop reliable methods for predicting the expected seismic displacement demand. Full-scale testing is required to confirm the hysteretic response of the rocking pier system that was assumed in the numerical simulations. Shake table tests should also be conducted to experimentally verify the interaction between column rocking response and the vertical dynamic vibration of the superstructure.

ACKNOWLEDGMENTS

The authors acknowledge the support from the Natural Sciences and Engineering Research Council of Canada (NSERC), the Canadian Institute of Steel Construction (CISC), Toronto, ON, Rapid Span Structures Ltd., Armstrong, BC, and S-Frame Software, Inc., Richmond, BC.

REFERENCES

- [1] Skinner, R.I., Tyler, R.G., Heine, A.J., and Robinson, W.H. (1980). "Hysteretic dampers for the protection of structures from earthquakes." *Bulletin of the New Zealand National Society for Earthquake Engineering*, 13(1), 22-36.
 - [2] Dowdell, D., and Hamersley, B. (2000). "Lions' Gate Bridge North Approach – Seismic Retrofit," *Proceedings of the Third International STESSA 2000 Conference*, Montreal, QC, Canada. 319-326.
 - [3] Routledge, P.J., Cowan, M.J., and Palermo, A. (2016). "Low-damage detailing for bridges - A case study of Wigram-Magdala Bridge." *Proceedings of the 2016 NZSEE Conference*, New Zealand Society for Earthquake Engineering, Wellington, New Zealand.
 - [4] Mander, J., and Cheng, C. (1997). *Seismic resistance of bridge piers based on damage avoidance design*. Technical Report No. NCEER-97-0014, State University of New York at Buffalo, Buffalo, NY.
 - [5] Hewes, J.T., and Priestley, M.J.N. (2002). Seismic design and performance of precast concrete segmental bridge columns, Report No. SSRP-2001/25, Department of Structural Engineering, University of California, San Diego, CA.
 - [6] Palermo A, Pampanin S, and Marriott D. (2007). "Design, modelling and experimental response of seismic resistant bridge piers with posttensioned dissipating connections." *Journal of Structural Engineering*; 133(11), 1648-1662.
 - [7] Marriott, D., Pampanin, S., and Palermo, A. (2009). "Quasi-static and Pseudo-Dynamic Testing of Unbonded Post-tensioned Rocking Bridge Piers with External Replaceable Dissipaters." *Earthquake Engineering and Structural Dynamics*, 38(3), 331-354.
 - [8] Mashal, M. and Palermo, A. (2014). "Quasi-Static Cyclic Tests of Half-Scale Fully Precast Bridge Bents Incorporating Emulative and Post-tensioned Low Damage Solutions, Second European Conference on Earthquake Engineering and Seismology, Istanbul, 25-29 August 2014
 - [9] Pollino, M., and Bruneau, M. (2010). "Seismic Testing of a Bridge Steel Truss Pier Designed for Controlled Rocking." *Journal of Bridge Engineering*, 136(12), 1523-1532.
 - [10] Guerrini, G., Restrepo, J.I., Massari, M., and Vervelidis, A. (2014). "Seismic Behavior of Posttensioned Self-Centering Precast Concrete Dual-Shell Steel Columns." *Journal of Structural Engineering*, 141(4), DOI: 10.1061/(ASCE)ST.1943-541X.0001054.
 - [11] Freddi, F., Dimopoulos, C.A., Karavasilis, T. (2017). "Rocking damage-free steel column base with friction devices: design procedure and numerical evaluation." *Earthquake Engineering and Structural Dynamics*, DOI: 10.1002/eqe.2904.
 - [12] Rahmzadeh, A.M., Alam, S., and Tremblay, R. (2018). "Finite Element Analysis of the Cyclic Response of Rocking Steel Bridge Piers with Energy Dissipating Steel Bars." *Journal of Structural Engineering*, 144(11), DOI: 10.1061/(ASCE)ST.1943-541X.0002216.
 - [13] CSA. (2014). *CSA S6-14, Canadian Highway Bridge Design Code*, Canadian Standards Association (CSA), Toronto, ON.
 - [14] CSI. (2018). *SAP2000 Ultimate – Structural Analysis Program*. Computers and Structures, Inc. (CSI), Berkeley, CA.
- NRCC. (2017). *Structural Commentaries (User's Guide – NBC 2015: Part 4 of Division B)*, 4th ed., National Research Council of Canada (NRCC), Ottawa, ON.